

Pattern motion is present in V1 of awake but not anaesthetized monkeys

Kun Guo*, Philip J. Benson† and Colin Blakemore

University Laboratory of Physiology, University of Oxford, Oxford OX1 3PT, UK

Keywords: monkey, motion selectivity, pattern motion, striate cortex

Abstract

We compared responses of neurons, recorded in striate cortex (area V1) of awake, fixating monkeys, to a single drifting grating with those to a 'plaid' pattern comprised of two superimposed drifting gratings separated in orientation by 90°. Five out of 54 (9%) of V1 direction selective neurons responded to the direction of motion of the whole pattern [pattern motion (PM) selectivity]. Tuning curves for plaid stimuli were similar in both optimum direction and width of tuning to those for single gratings. Twenty nine out of 54 (54%) responded simply to the motion of individual orientated gratings within the pattern [component motion (CM) selectivity]. The remaining 37% (20/54) neurons were unclassified. In control experiments, 39 direction selective neurons were recorded in area V1 of anaesthetized monkey and cats. Unlike area V1 in behaving monkeys, none of these neurons exhibited PM selectivity to the drifting plaids. Twenty eight out of 39 (72%) of them responded to the direction of the component gratings and were classified as CM selectivity. Our results indicate that although most V1 neurons are CM selective, as described in anaesthetized animals, a subpopulation is clearly PM selective in behaving monkeys, reflecting integration of locally derived motion signals. Neurons in V1 therefore carry signals that may contribute to pattern motion processing and perception. This perceptual interpretation in V1 might depend much more critically on information integration mechanisms that only function properly in awake, perceiving animals.

Introduction

In the primate brain, motion information is processed in a hierarchical manner. Psychophysical evidence suggests that at the earlier stage of motion processing, mechanisms selective for orientation and spatial frequency compute motion signals within localized regions of visual space. These signals are then combined according to simple geometric rules at the later stage of motion processing where the direction and velocity of complex moving objects are represented (Adelson & Movshon, 1982; Adelson & Bergen, 1985; Ferrera & Wilson, 1990). Electrophysiological recordings from anaesthetized monkeys have revealed potential correlates of these two stages in striate cortex (area V1) and extrastriate middle temporal area (area MT), respectively. In area V1, direction selective neurons are generally selective for component motion (CM). They respond maximally to the direction of stimulus movement orthogonal to the preferred orientation (Schiller *et al.*, 1976); this direction is not necessarily the same as the motion of entire object or surface, of which the neuron's preferred contour is only a small component (Movshon *et al.*, 1985; Movshon & Newsome, 1996). On the other hand, populations of MT neurons are pattern motion (PM) selective,

integrating motion direction vectors from various edges in an object into a more global representation of the true direction of object motion (Movshon *et al.*, 1985; Rodman & Albright, 1989). Therefore, area MT provides a second stage analysis of signals from area V1 (Salzman *et al.*, 1990; Snowden, 1994; Stoner & Albright, 1994; Andersen, 1997).

In addition to the feedforward and lateral inputs, a cortical neuron receives feedback inputs from areas presumed to be higher in the assumed serial hierarchy (Gilbert, 1998; Barone *et al.*, 2000). The density of such back-projections (sometimes involving as many axons as in the feedforward pathway) suggests that they play important functions to shape neural representations in lower visual areas, such as informing lower visual areas of the results of processing in higher areas, especially when those higher computations involve analysis of a wider range of features or a larger area of visual field than is available directly within the receptive fields (RFs) of neurons in lower areas (Hochstein & Ahissar, 2002).

Over 90% of the back-projections from MT target V1 and terminate in layer 4B (Maunsell & Van Essen, 1983; Shipp & Zeki, 1989), which contains populations of CM selective neurons that provide the forward-projecting inputs to MT (Movshon & Newsome, 1996). We propose, then, that the computed properties of PM selectivity might be fed back to neurons in V1 under conditions in which corticocortical connections are operational in the conscious host. By comparing responses of neurons to a single drifting grating with those to a 'plaid' pattern comprised of two superimposed drifting gratings, the stimuli conventionally employed to differentiate CM and PM selectivity (Movshon *et al.*, 1985), we investigate whether V1 neurons in layer 4B (and layer 6, where neurons also receive back-projections from MT) exhibit PM selectivity in awake, fixating monkeys.

Correspondence: Dr Philip J. Benson, at †present address below.
E-mail: psy317@abdn.ac.uk

*Present address: School of Biology, University of Newcastle, Newcastle upon Tyne, NE2 4HH, UK

†Present address: School of Psychology, College of Life Sciences and Medicine, William Guild Building, King's College, University of Aberdeen, Old Aberdeen, AB24 2UB, UK

Received 29 August 2003, revised 10 November 2003, accepted 16 December 2003

Materials and methods

Animal training and preparation for awake recording

Two adult male rhesus monkeys (*Macaca mulatta*, 7.5–8.5 kg) were trained to fixate a small fixation point (FP) for several seconds in a dimming fixation detection task (Guo & Benson, 1998). Once they learned the task, a scleral eye coil (Judge *et al.*, 1980), head restraint and a recording chamber positioned over occipital lobe to provide access to central visual field representation in area V1 were implanted under deep anaesthesia (Isoflurane delivered via endotracheal intubation by nitrous oxide and oxygen transport) and aseptic conditions (Guo & Benson, 1998). All procedures complied with UK Home Office regulations on animal experimentation [Animals (Scientific Procedures) Act, 1986].

During the experiment, the monkeys sat in a primate chair with head restrained and binocularly viewed a display placed at 57 cm in front of their eyes, subtending a visual area of $32 \times 24^\circ$. Their eye movements were monitored by a 3-foot³ scleral search coil assembly (R3FTCL-A, CNC Engineering). A computer-controlled fixation window of $\pm 1^\circ$ was used. The luminance of the FP and uniform grey background were 50 and 15 cd/m², respectively. Trials were initiated when the animal pressed a lever attached to the chair. Initially, a 0.2° FP was presented in the centre of screen. After a 500 ms delay, a visual stimulus (moving bar, grating or plaid) that varied in size and position was also presented. The monkeys were required to maintain fixation without reacting to other visual stimulation. If they disengaged fixation the trial was aborted automatically. The FP dimmed (30% contrast) after a random period of 1–6 s. The monkeys had to release the lever within 400 ms of dimming in exchange for water reward. The intertrial interval was 1500 ms.

Animal preparation for acute recording

Standard electrophysiological techniques for extracellular recording were used for two adult cats (3.2–3.8 kg) and one adult cynomolgus monkey (2.5 kg) (Scannell *et al.*, 1996). The animals were initially anaesthetized with ketamine (10 mg/kg). General anaesthesia was carried out using halothane (1–3%) and a 70:30 mixture of nitrous oxide and oxygen. During the recording, the animals were paralyzed with a continuous intravenous infusion of pancuronium bromide (0.1 mg/kg/h) in glucose-saline and artificially ventilated. The rectal temperature ($\sim 38^\circ\text{C}$), expired CO₂ (3.5–4.5%), electrocardiogram and electroencephalogram were continuously monitored and maintained. A small craniotomy was positioned over the area V1.

Pupils were dilated with atropine and nictitating membranes were retracted with phenylephrine hydrochloride (2.5%). The corneas were protected with zero-power contact lenses and artificial pupils (3 mm diameter) were positioned in front of each eye. The refractive state of each eye was measured by direct ophthalmoscopy, and additional lenses were used to focus the eyes on the stimulus monitor.

Visual stimulation and data collection

Visual stimuli (sinusoidal gratings and plaids) were generated by VSG 2/3 W graphics system (Cambridge Research Systems) and displayed on a gamma-corrected high frequency noninterlaced colour monitor (110 Hz, Iiyama MF8617e, Graphics Direct). Additive plaids comprised two superimposed component gratings with same contrast, spatial and temporal frequency, but separated by 90° in orientation. Such a plaid is normally perceived by human (Movshon *et al.*, 1985) and monkey observers (Thiele & Stoner, 2003) as moving in a single direction, corresponding to the shared vector of motion of two component gratings (the bisector of the two directions if their velocities are identical).

The activity of V1 single and multiunits was recorded using parylene-insulated tungsten microelectrodes (1–2 M Ω impedance). Single neuron activity was determined on the basis of constant amplitude and waveform. Having isolated a neuron, its RF was mapped using a sinusoidal grating patch moving across the screen with variable length, width and velocity. Within the patch, the optimal grating drifted continuously in the neuron's preferred direction. In this way, we estimated RF width and breadth profiles as well as optimal orientation, direction, spatial and temporal frequency. A drifting sinusoidal grating or plaid was then positioned in the RF centre and presented through a circular 8° annulus for 1 s. Each stimulus was presented in 16 directions of motion with a constant angular deviation (22.5°). Spatial (0.5–4 cycles/deg) and temporal frequency (1–8 Hz) of the gratings were optimal for the neuron. To avoid over-modulating the plaids, only moderately high contrast (30–50%) was used for the gratings. Each condition was presented 5–10 times and presentation order was randomised to counter repetition effects.

Data analysis

The neuron's discharge for the duration of stimulus presentation was averaged and normalized after the recording. The RF of each neuron recorded was classified as simple or complex on the basis of the spatial arrangement of 'on' and 'off' regions and the presence of spatial summation within each region (Hubel & Wiesel, 1962). These classifications were later confirmed by the frequency component of their responses to the optimal drifting sinusoidal grating (Skottun *et al.*, 1991). We recorded preferentially from complex cells for the following reasons: (i) previous results about the CM/PM selectivity in area V1 of macaque were mainly based on the complex cells (Movshon & Newsome, 1996); (ii) complex cells tend to be more direction selective than simple cells (Hubel & Wiesel, 1968; Conway & Livingstone, 2003); (iii) simple cells are sensitive to variations in spatial phase of the drifting gratings and plaids (Gizzi *et al.*, 1990; Carandini, Heeger & Movshon, 1997). However, it is difficult to ensure the constant phase of the gratings throughout the trials in the awake recordings due to small fixational eye movements, and this could affect their relative preference for component and pattern motion. Previous studies showed that there was no evident CM/PM selectivity difference among V1 neurons that depended on their RF type (Gizzi *et al.*, 1990). When analysing neuronal responses to drifting gratings and plaids, mean firing rates were used for complex cells. For simple cells the modulation in firing at the stimulus temporal frequency was used (Carandini *et al.*, 1997; Tinsley *et al.*, 2003). To exclude the possible phase variation effect on simple cells, we also calculated a symmetry index (SI):

$$\text{SI} = (\text{Dc1} + \text{Dp}) / (\text{Dc2} + \text{Dp}),$$

where Dp is the neural response to the plaid drifting in its preferred direction (as determined by its responses to single gratings), Dc1 and Dc2 are the two response values (Dc1 < Dc2) obtained when the plaid drifted in the two directions such that one of the component gratings drifted in the neuron's preferred direction. Any simple cells with a symmetry index of <0.85 were excluded from the analysis (Tinsley *et al.*, 2003).

Neurons that were highly responsive to drifting gratings were submitted to single-factor analysis of variance (ANOVA) to determine orientation/direction selectivity. Directional selectivity was characterized by a direction index (DI):

$$\text{DI} = 1 - N/P,$$

where P and N are the neuron's firing rate to motion in its preferred and opposite directions (each minus spontaneous firing rate). Neurons with no direction preference will give equal responses in both directions and

have a DI of 0. A unidirectional neuron gives an index near 1, and a neuron inhibited by motion in the null direction gives a value >1 . Direction selective neurons were selected from the sample that yielded significant terms in analysis of variance, and had a DI >0.5 (DeValois *et al.*, 1982; Hawken *et al.*, 1988; Chaudhuri & Albright, 1997).

Neurons tested with both grating and plaid stimuli were classified as CM or PM selective by comparing the actual responses to a plaid with the responses predicted from the responses to a grating (the responses of an idealized component neuron and an idealized pattern neuron) (Movshon *et al.*, 1985). For the calculation of the component prediction, the spontaneous firing rate was subtracted from the responses to the gratings before they were added together, and added back after the prediction has been computed. To quantify the degree of correspondence between experimentally measured plaid tuning curve and predicted tuning curve for CM and PM selectivity, partial correlation coefficients for pattern (R_p) and component (R_c) prediction were calculated as follows (Movshon & Newsome, 1996):

$$R_p = \frac{r_p - r_c r_{pc}}{\sqrt{(1 - r_c^2)(1 - r_{pc}^2)}} \quad \text{and}$$

$$R_c = \frac{r_c - r_p r_{pc}}{\sqrt{(1 - r_p^2)(1 - r_{pc}^2)}}$$

where r_c is the raw correlation of the data with the component prediction, r_p the raw correlation of the data with the pattern prediction, and r_{pc} the correlation of the two predictions.

R_p and R_c were used to classify each neuron as PM or CM selective, or neither; and were presented in a scatterplot (see Fig. 1E for an example). The 'component' zone contains values of R_c that are significantly greater than either R_p or 0. The 'pattern' zone contains values of R_p that are significantly greater than either R_c or 0. The zone marked 'unclassified' contains neurons for which neither R_c or R_p significantly exceed 0, or are greater than 0 but no different from one another (Movshon *et al.*, 1985; Gizzi *et al.*, 1990). The significance of differences between R_p and R_c were indicated by a parametric statistical value t and calculated as:

$$t = \frac{Z_p - Z_c}{\sqrt{2/(n-3)}}$$

in which

$$Z_x = \frac{1}{2} \ln \frac{1 + R_x}{1 - R_x},$$

for $x = p$ and c , and $n = 16$.

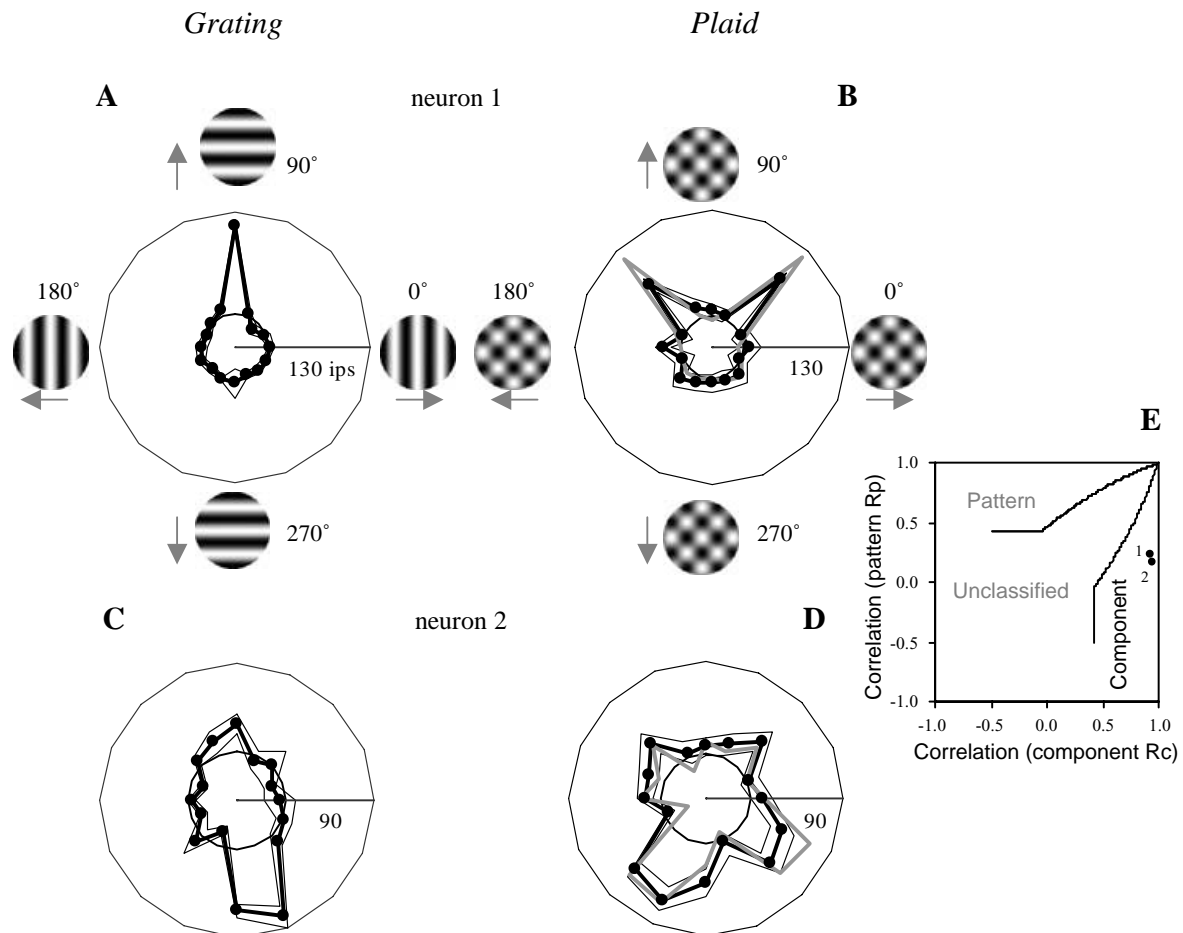


FIG. 1. Directional tuning curves of two CM selective neurons, sampled from area V1 of behaving monkeys, to drifting gratings (A and C) and plaids (B and D). Each polar plot (black solid line) shows neuron's responses to 16 directions of motion (grating or plaid) with a constant angular deviation (22.5°). Thin black lines indicate standard error of the mean. The radial co-ordinate represents mean firing rate (spikes/s) and the polar angle corresponds to the direction of displacement. Spontaneous firing rate is indicated by a solid small circle. Grey solid lines in B and D indicate predicted tuning curve should the neuron respond only to the direction of two component gratings within the plaid (component prediction). E shows scatter plot diagram of the two neurons' directional selectivity (filled circles 1 and 2). The bullet-shaped contour divides the space, within which the category data lays, into component, pattern and unclassified zones based on computed R_p and R_c (for details see data analysis section in Methods section).

Results

Two hundred and twelve V1 neurons, spanning a range of visual field eccentricities from 0.5° to 10° , were recorded from three hemispheres of two awake, fixating monkeys. 60 neurons were classified as direction selective (mean \pm SD $DI = 0.79 \pm 0.21$), 103 neurons were orientation selective (ANOVA, $P < 0.05$) and the remaining 49 neurons were nonoriented.

Although it is difficult to determine the laminar locations of neurons in behaving monkey experiments (these animals were being used in other experiments), we could estimate the location of sampled neurons according to following criteria: (i) recorded depths of electrode entrances to, and exits from, grey matter; (ii) recorded depths of physiologically recognizable landmarks such as high spontaneous activity and concentration of nonoriented neurons of layer 4C (Dow, 1974). As in previous reports (Hawken *et al.*, 1988; Orban, 1994), we have good reason to believe that all direction selective neurons recorded in our experiment were located in the deeper cortical layers 4 and 6.

Responses of direction selective neurons to gratings and plaids in behaving monkeys

Fifty-four V1 complex direction selective neurons were tested by both grating and plaid stimuli, and classified as CM or PM selectivity. Figure 1 shows polar plots of direction tuning to drifting gratings and plaids of two CM selective neurons from the sample. When stimulated by a sinusoidal grating which was moved in 16 directions through their RFs, neuron 1 responded best to upward motion ($DI = 0.96$) with a tuning bandwidth of 26° (Fig. 1A), while neuron 2 had maximum discharge to nearly downward motion ($DI = 0.81$) with 48° tuning bandwidth (Fig. 1C). The black solid curves and symbols in Fig. 1B and D illustrate direction tuning curves of these two neurons to a drifting plaid comprising two sinusoidal gratings separated in orientation by 90° . The labelled directions on the polar plot correspond to the direction of motion of the plaid. For a plaid moving upwards, one of the component gratings moved up and to the right while the other one moved up and to the left. If these neurons responded to the direction of global motion (PM selective), their direction tuning curves for the plaid would have been essentially the same as that for the single grating, with a single peak for upward or downward motion. If, on the other hand, the neurons encoded the direction of the component gratings (CM selective), they should respond equally and maximally to two different directions of the plaid drift, at which each of the component gratings appears at the optimal direction in their RFs. The tuning curves for the plaid should have confirmed to the predicted tuning curves (grey solid lines in Fig. 1B and D), which were calculated simply from the sum of two tuning curves expected if the neurons responded independently to each of the component gratings. As shown in Fig. 1B and D, the direction tuning curves for the drifting plaids of these neurons corresponded better to the curves expected for CM rather than PM selectivity. With high partial component correlations (neuron 1, $R_c = 0.95$, $R_p = 0.16$; neuron 2, $R_c = 0.92$, $R_p = 0.23$), they were unambiguously classified as CM selective (Fig. 1E).

Although most of the V1 neurons exhibited CM selective to the drifting plaids, five of them did respond to the global direction of entire pattern motion (Fig. 2). Taking neurons 3 and 4 as examples, for the drifting gratings, their preferred directions were downward ($DI = 0.68$, Fig. 2A) and rightward ($DI = 0.8$, Fig. 2C) with tuning bandwidths of 27° and 35° . For the drifting plaids, unlike the CM selective neurons shown in Fig. 1, these two neurons had larger responses when the

plaids drifted in their preferred direction ('pattern response') than when either of two component gratings drifted in the same direction ('component responses'). Their direction tunings for the plaids showed single downward or rightward peak with tuning bandwidths of 28° and 35° (solid lines in Fig. 2B and D) that approximates pattern prediction. With high partial pattern correlations and low partial component correlations (neuron 3, $R_p = 0.77$, $R_c = 0.31$; neuron 4, $R_p = 0.9$, $R_c = 0$), they were classified as PM selective (Fig. 2K).

Figure 3 shows direction tuning curves for three neurons that could not be classified as either CM or PM selective. These neurons showed clear direction preference for the drifting gratings ($DI = 0.66$, 0.85 and 0.66 for neurons 8, 9 and 10 in Fig. 3A, C and E), but their responses to the drifting plaids did not correlate well with either pattern or component prediction (Fig. 3B, D and F). As their partial pattern correlations ($R_p = 0.62$, 0.78 and 0.71 for neurons 8, 9 and 10) and partial component correlations ($R_c = 0.79$, 0.84 and 0.5) did not differ significantly from one another, they were termed 'unclassified' neurons (Fig. 3G). In accordance with previous reports (Movshon *et al.*, 1985; Rodman & Albright, 1989), most of these neurons in our sample had broad and/or ragged direction tuning curves for the drifting gratings.

The computed R_p and R_c of all tested V1 direction selective neurons from behaving monkeys are presented in a scatter plot within which neurons can be categorized within component, pattern or unclassified zone (Fig. 5A). Out of 54 neurons quantified in this way, five neurons (9%) were classified as PM selective. Their direction tuning curves for the drifting plaids were similar in direction and breadth of tuning as that for the single gratings. Twenty nine neurons (54%) were CM selective. Their responses to the drifting plaids corresponded well with the component prediction, but poorly to the pattern prediction. The remaining 20 neurons (37%) were unclassified. Interestingly, neurons showing PM selectivity to the drifting plaids were all recorded in the layer very close to 4C (probably 4B), while no clear pattern of laminar distribution (layers 4 or 6) was observed for CM and unclassified neurons.

Responses of direction selective neurons to gratings and plaids in anaesthetized animals

We repeated our recording in area V1 of one anaesthetized monkey and two anaesthetized cats. When tested with the drifting gratings, 39 complex cells were classified as direction selective neurons ($DI = 0.64 \pm 0.11$). All of them failed to retain any discernible form of PM tuning when tested with the drifting plaids, although most of them responded to the direction of individual component gratings within the plaids. Figure 4 shows direction tuning curves of two CM selective neurons. These neurons showed clear direction preference to single grating drifted through their RFs ($DI = 0.7$ and 0.73 for neurons 11 and 12 in Fig. 4A and C). For the drifting plaids, they responded maximally when either of the component gratings drifted in their preferred direction rather than the whole plaid pattern (Fig. 4B and D). Their direction tuning curves correlated well with the component prediction (neuron 11, $R_c = 0.91$, $R_p = -0.11$; neuron 12, $R_c = 0.94$, $R_p = 0.38$), and they were classified as CM selective.

Population data from the anaesthetized animals is also plotted as a scatter plot of partial correlation coefficients (Fig. 5B). Out of 39 neurons, 28 (72%) were clearly classified as CM selective. They had significant individual direction tuning for the orientated component gratings that formed plaid stimulus, and their tuning curves matched up well with the component prediction. The remaining 11 neurons (28%) fell within the 'unclassified' portion, their responses to the drifting plaids correlated to neither component nor pattern prediction. No PM selective neuron was observed.

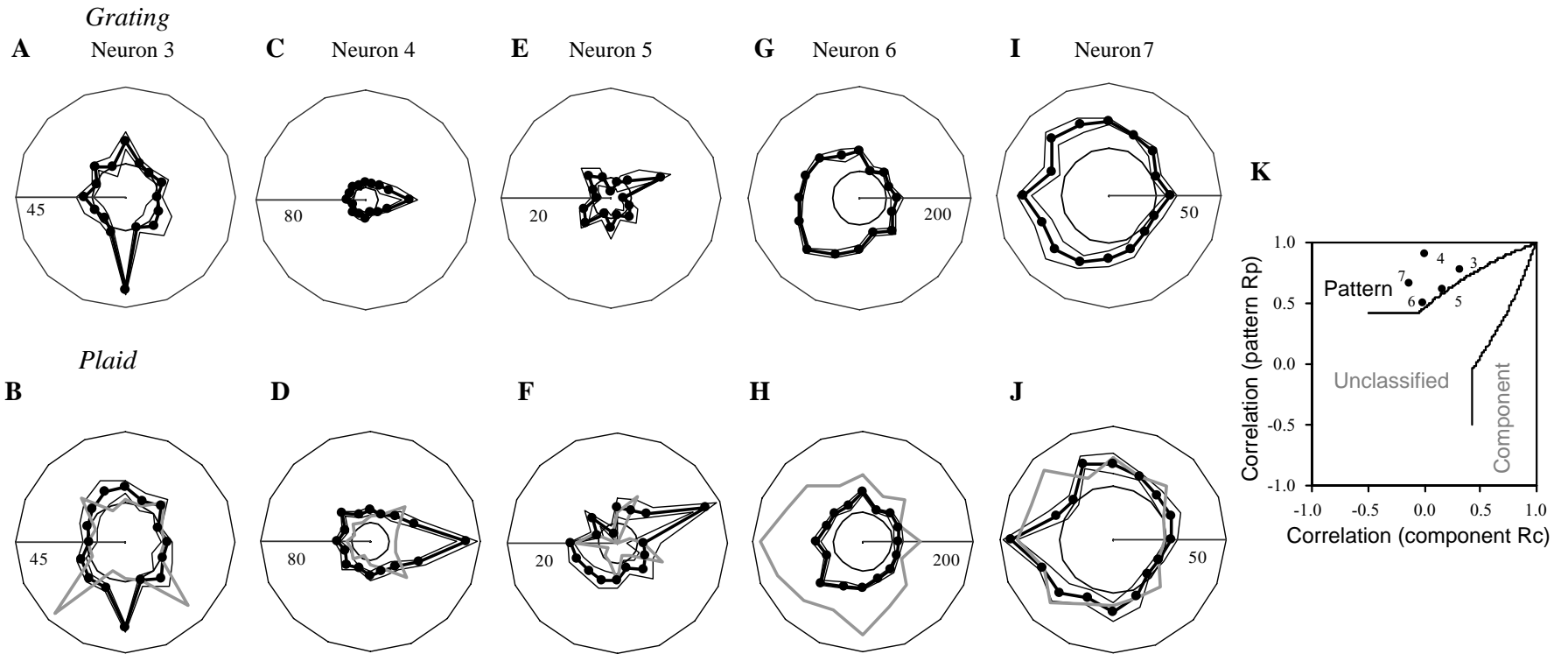


FIG. 2. Directional tuning curves of five PM selective neurons, sampled from area V1 of behaving monkeys, to drifting gratings (A, C, E, G and I) and plaids (B, D, F, H and J). The scatter plot diagram of directional selectivity of these five neurons is shown in K.

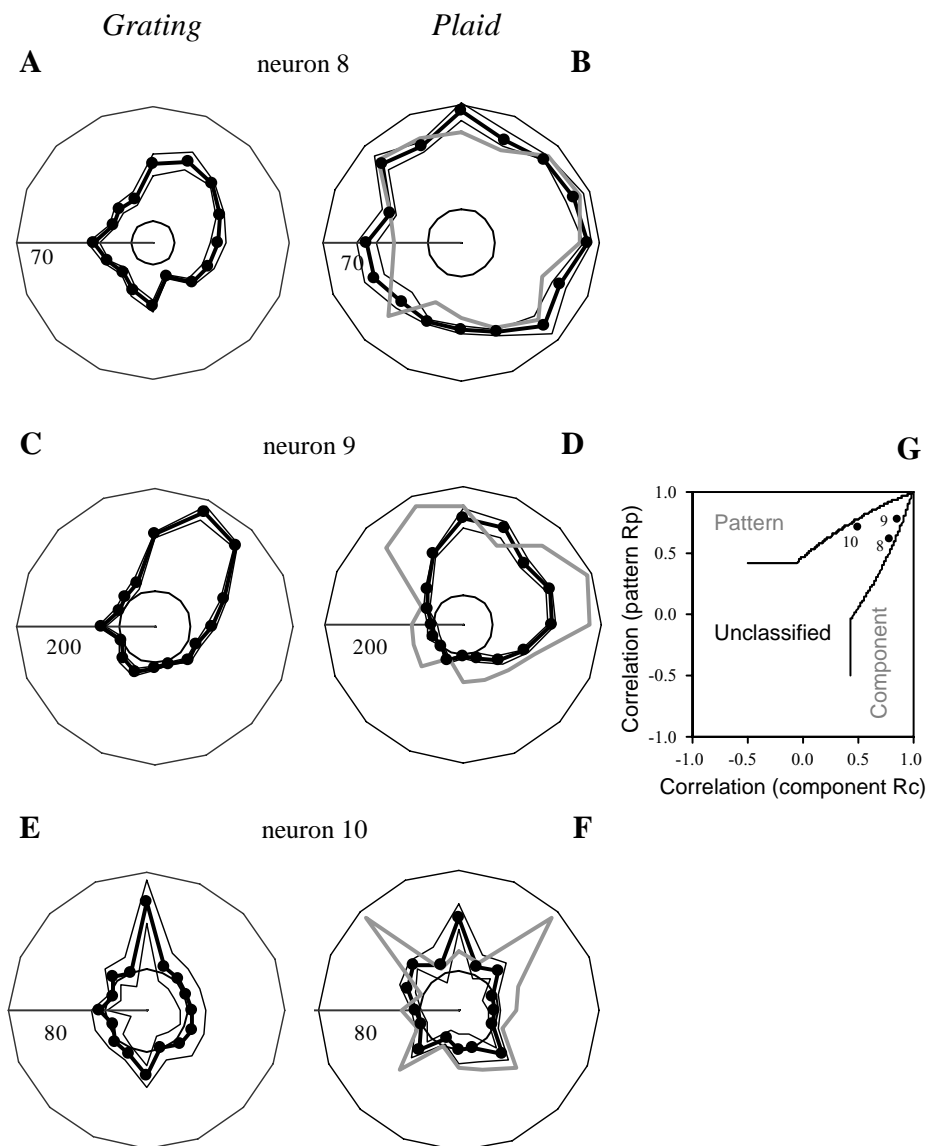


FIG. 3. Directional tuning curves of three unclassified neurons, recorded from area V1 of behaving monkeys, to drifting gratings (A, C and E) and plaids (B, D and F). The scatter plot diagram of these neurons' directional selectivity is shown in G.

From the population results shown in Fig. 5A and B, it seems that V1 neuron responses to the pattern motion are different between awake and anaesthetized animals. Indeed, two-dimensional Kolmogorov-Smirnov analysis revealed a significant difference in the distribution of neurons' partial correlation coefficients between awake and anaesthetized animals ($P < 0.01$). As our anaesthetized samples were from one monkey and two cats, to exclude unlikely species difference, we compared our V1 samples from awake macaques with Movshon & Newsome's (1996) V1 samples from anaesthetized macaques (indicated by \times in Fig. 5B). The distribution of R_p and R_c was still significantly different between V1 samples from awake and anaesthetized macaques ($P < 0.01$), but no difference was observed between our anaesthetized V1 sample and Movshon and Newsome's V1 sample ($P > 0.05$). We further compared our data with anaesthetized MT samples from Movshon's report (Movshon *et al.*, 1985; Fig. 5C). The difference of neurons' R_p and R_c distribution was significant between awake V1 and anaesthetized MT ($P < 0.01$), the not between V1 neurons sampled in layer 4B and MT neurons ($P = 0.02$).

Responses of bi-direction selective neurons to grating and plaid stimuli

With direction selective neurons, we also compared the responses to the drifting gratings and plaids of some V1 bi-direction selective ($DI < 0.5$, orientation selective) neurons (3 simple cells and 87 complex cells), sampled from the awake, fixating monkeys. R_p and R_c were computed using the largest responses within either the $0-180^\circ$ or $180-360^\circ$ direction tuning range, as these two ranges are effectively the same.

Some bi-direction selective neurons could discriminate the component gratings within the plaid and consequently responded to different direction/orientation of the component gratings as they did to the single grating. Figure 6 shows two examples. Tested with the drifting gratings, neurons 13 and 14 had clear bi-directional preference with preferred direction of vertical (Fig. 6A; $DI = 0.04$) and horizontal (Fig. 6C; $DI = 0.07$). When a plaid drifted diagonally, one of its component gratings drifted with each of these two neurons' preferred

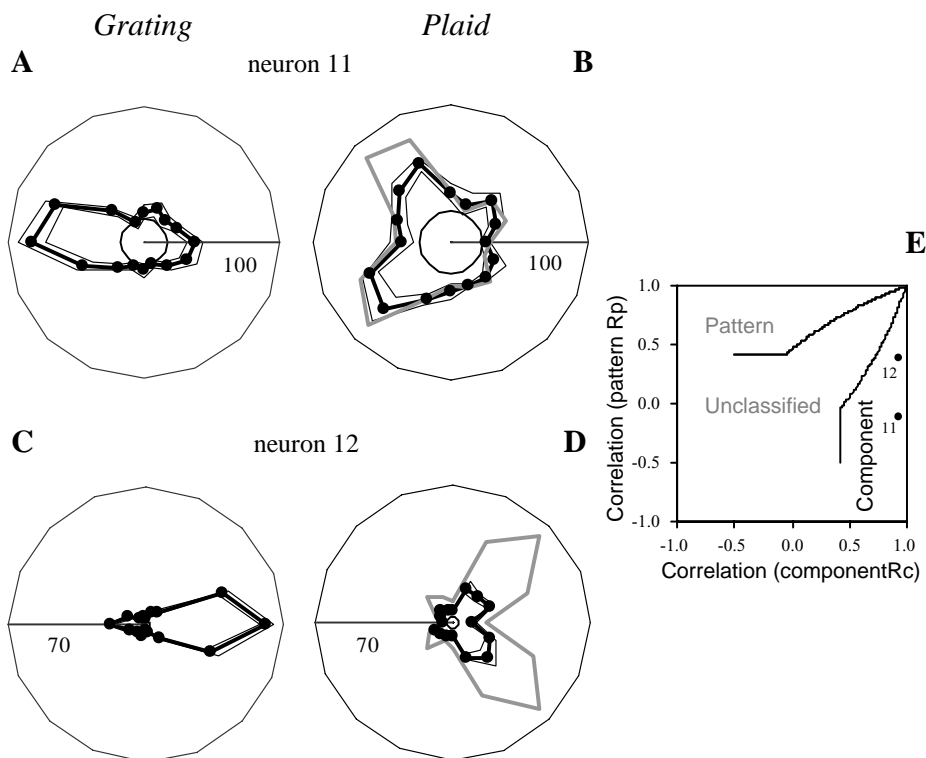


Fig. 4. Directional tuning curves of two CM selective neurons, sampled from area V1 of anaesthetized monkeys, to drifting gratings (A and C) and plaids (B and D). The scatter plot diagram of two neurons' directional selectivity is shown in E.

(horizontal or vertical) direction, and elicited peak responses from both neurons (Fig. 6B and D). Correlating well with the component prediction (neuron 13, $R_c = 0.98$, $R_p = -0.02$; neuron 14, $R_c = 0.73$, $R_p = -0.37$), these two neurons were classified as CM selective (Fig. 6E).

Although having clear bi-directional preference for the single grating, some V1 neurons failed to retain direction/orientation tuning predicted by CM selectivity for the plaid stimulus. Shown in Fig. 7, neurons 15 and 16 demonstrated preference for horizontal (Fig. 7A; $DI = 0.38$) and diagonal (Fig. 7C; $DI = 0.17$) direction for the drifting gratings. Their tuning curves for the drifting plaids, however, were not well correlated with the component prediction (Fig. 7B and D). Without distinguishable R_p and R_c (neuron 15: $R_c = 0.2$, $R_p = -0.05$; neuron 16: $R_c = -0.32$, $R_p = 0.3$), they were put into the unclassified category (Fig. 7E).

Population results revealed that out of 90 bi-direction selective neurons tested, 57 neurons (63%) were CM selective. They had similar direction/orientation tuning curves for the single grating and the component gratings formed plaid stimuli. The remaining 33 neurons (37%) were unclassified (Fig. 8).

Clearly, no bi-direction selective neurons demonstrated PM selectivity to the drifting plaids in our experiment, where some direction selective neurons did. To examine whether there is a relationship between a neuron's direction selectivity (measured with the drifting gratings) and pattern motion selectivity (measured with the drifting plaids), we calculated a pattern index, which describes the strength of pattern selectivity relative to component selectivity, for each neuron. The pattern index is obtained by subtracting the variance accounted for by the component prediction from that accounted for by the pattern prediction ($R_p^2 - R_c^2$) (Stoner & Albright, 1992; Pack *et al.*, 2001). Positive values indicate close conformity with the pattern prediction, while negative values support the component prediction. The scatter

plot of the pattern index against the direction index for each neuron did not show a significant systematic shift to PM selectivity with increasing direction selectivity for the population data ($r^2 = 0.04$, Fig. 9).

Bandwidth comparison for direction/bi-direction selective neurons

We compared the neurons' direction tuning bandwidths to the drifting gratings and plaids, and did not observe significant difference between two stimuli. The mean bandwidths obtained with the drifting gratings and plaids were $35.4 \pm 18^\circ$ and $34 \pm 14.2^\circ$ for bi-direction selective neurons with CM selectivity (paired *t*-test, $P = 0.33$), and were $48.9 \pm 26.2^\circ$ and $46.7 \pm 25.9^\circ$ for direction selective neurons with CM or PM selectivity ($P = 0.32$).

We also noticed that direction selective neurons ($55.8 \pm 31.8^\circ$) generally have slightly broader tuning bandwidth (by a factor of ~ 1.25) to the drifting gratings than bi-direction selective neurons ($44.6 \pm 20.7^\circ$) (*t*-test, $P < 0.01$), which is consistent with previous observation (DeValois *et al.*, 1982).

Inhibition in orientation domain

Although the shape of tuning curves for responses to the drifting plaids can be predicted from the responses to the drifting gratings, most neuron responses to the plaids were smaller than the predicted (see Fig. 4B and D for examples). This we take to reflect inhibitory processes that operate in orientation domain (Blakemore & Tobin, 1972; Gizzi *et al.*, 1990). Our prediction for the CM responses did not take inhibition into account. The differences between the observed and predicted response magnitudes are most likely because of inhibition of the response to one grating by the presence of the other (cross-orientation inhibition). As a measure of this, we compared the measured peak response to the plaids (less spontaneous activity) with the predicted peak response. The majority of direction selective neurons

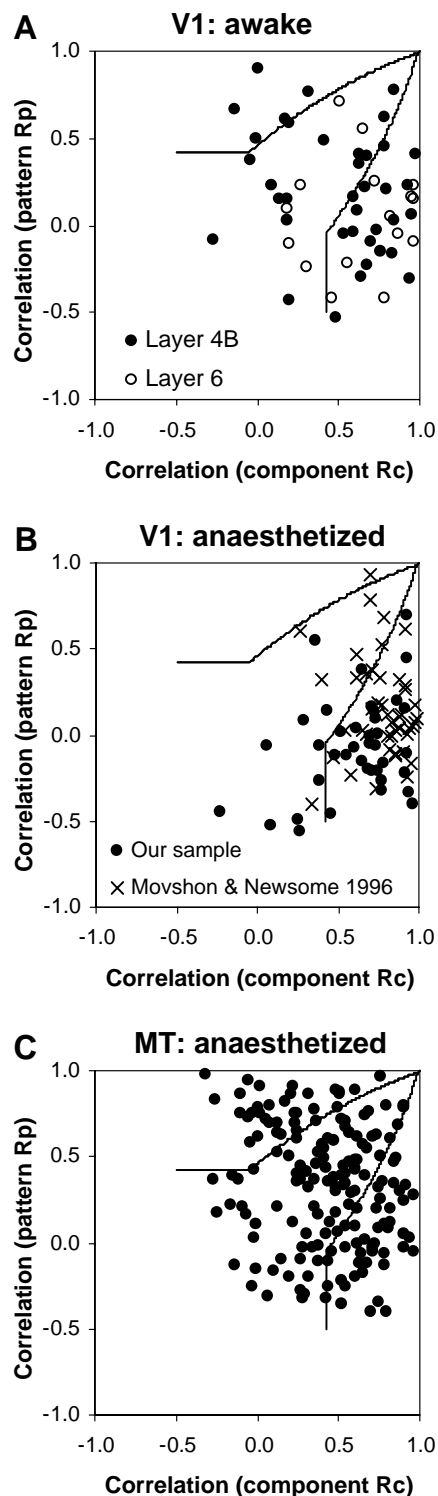


FIG. 5. Distribution of partial correlation coefficients (R_p and R_c) for V1 neurons in behaving monkeys (A), V1 neurons in anaesthetized animals (B), and MT neurons in anaesthetized monkeys (C). Some V1 samples in B (indicated by \times) come from Movshon & Newsome (1996), and MT samples in C are adapted from Movshon *et al.* (1985).

showed some sign of inhibition, especially for those recorded from anaesthetized animals. The mean ratios were 0.81 ± 0.32 and 0.65 ± 0.29 for neurons sampled from awake and anaesthetized animals, respectively. Similar results have also been observed in various

visual areas of anaesthetized animals (MT in monkeys, V1 and lateral suprasylvian cortex in cats; Movshon *et al.*, 1985; Gizzi *et al.*, 1990).

Control experiments

In the experiments described above, each of the component gratings within a plaid had the same contrast as the single grating used to test neuron's responses to the drifting gratings. As a result, the physical contrast of plaid stimuli was double that of grating stimuli, but the 'contrast per component' of all stimuli was identical (Gizzi *et al.*, 1990). For 13 neurons, we also recorded their responses to plaids composed of two gratings with half the contrast of a single grating, thus in the plaid pattern, the contrast between bright and dark 'blobs' at the intersections of individual bars of the component gratings matched the contrast of the single grating. In terms of direction selectivity, tests with half-contrast plaids yielded results that were no different with plaids having full contrast components. Similar results have already been reported by other researchers in our group (Scannell *et al.*, 1996).

Although we carefully monitored monkeys' eye position using a fixation window of $\pm 0.5^\circ$ or $\pm 1^\circ$ during data collection, small eye movements, such as microsaccade and micropursuit, unavoidably occurred during fixation. Previous observations suggest that these fixational eye movements could modulate the stimulus-related neural responses and largely account for response variability in area V1 of awake monkeys (Gur & Snodderly, 1997; Gur *et al.*, 1997; Martinez-Conde *et al.*, 2002). In our experiment, there was no systematic relation between the fixational eye movements and the neurons' direction selectivity to the drifting gratings and plaids. The preferred direction to the grating or plaid stimuli remained the same when we analysed data from time periods in which eye movements were absent or minimal. Figure 10 shows an example from neuron 4. As the motion onset can sometimes elicit early suppressed ocular following eye movements which normally occur within 200 ms after the motion onset (Guo & Benson, 1998, 1999), we compared this neuron's directional tuning to the drifting gratings and plaids using the discharges sampled from the whole period of motion presentation (0–1000 ms; black lines and symbols in Fig. 10), and from the time window between 200 and 1000 ms after the motion onset (grey lines and symbols in Fig. 10). Clearly, for both the drifting grating (Fig. 10A) and plaid stimuli (Fig. 10B), the neuron's preferred direction remained the same for different sampling windows, so did its PM selectivity (Fig. 10C).

Discussion

Research on brain mechanisms performing motion analysis has tended to illustrate serration in the hierarchical pathway for pattern motion analysis that includes areas V1, V2, V3 and MT. In anaesthetized monkeys, direction selective neurons in area V1, including neurons that project to MT directly, are generally 'orientation tuned' and CM selective signalling only the direction of movement orthogonal to the preferred orientation (Movshon *et al.*, 1985; Movshon & Newsome, 1996). In cytoarchitectonically distinct areas V2 and V3, studies have reported the existence of a small population of neurons exhibiting pattern-type behaviour (Gegenfurtner *et al.*, 1994; Stoner & Albright, 1994). To date, area MT is the only cortical region in primates currently known to contain a substantial population (around 1/3) of PM selective neurons that respond to the true direction of motion of complex patterns (Movshon *et al.*, 1985; Rodman & Albright, 1989; Stoner & Albright, 1992, 1994). Movshon *et al.* (1985) also indicated laminar segregation of different cell types in MT. PM neurons were primarily encountered in layers II, III and V (output laminae) and CM neurons were more often found in layers IV and VI (input laminae). As

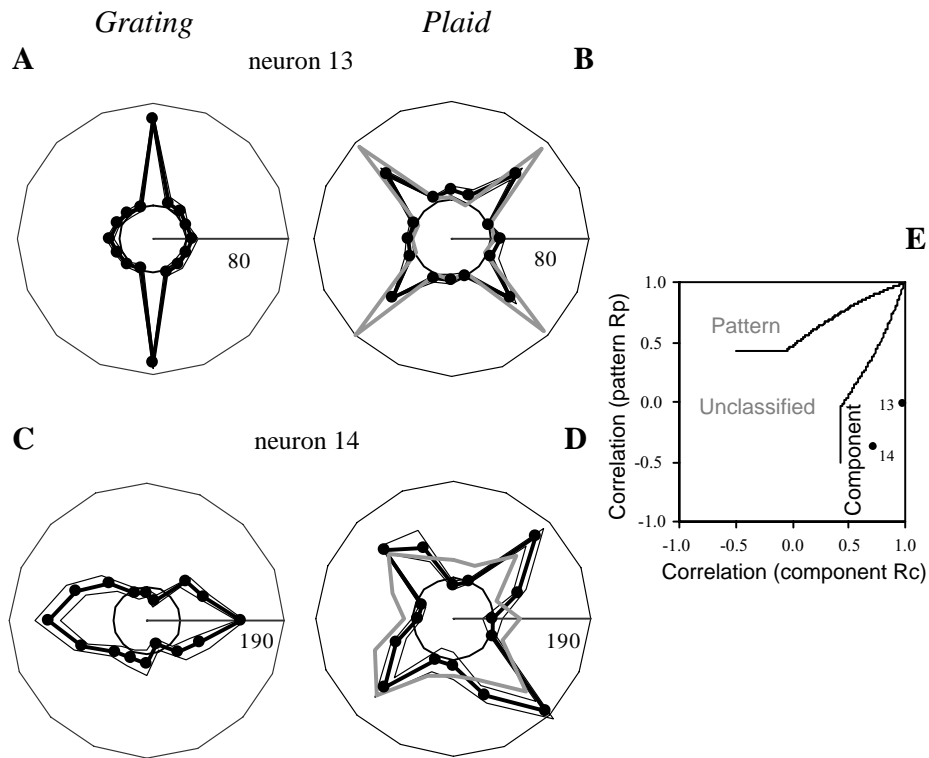


FIG. 6. Direction/orientation tuning curves to drifting gratings (A and C) and plaids (B and D) of two bi-direction selective neurons classified as CM selectivity. The scatter plot diagram of the distribution of two neurons' partial correlation coefficients is shown in E.

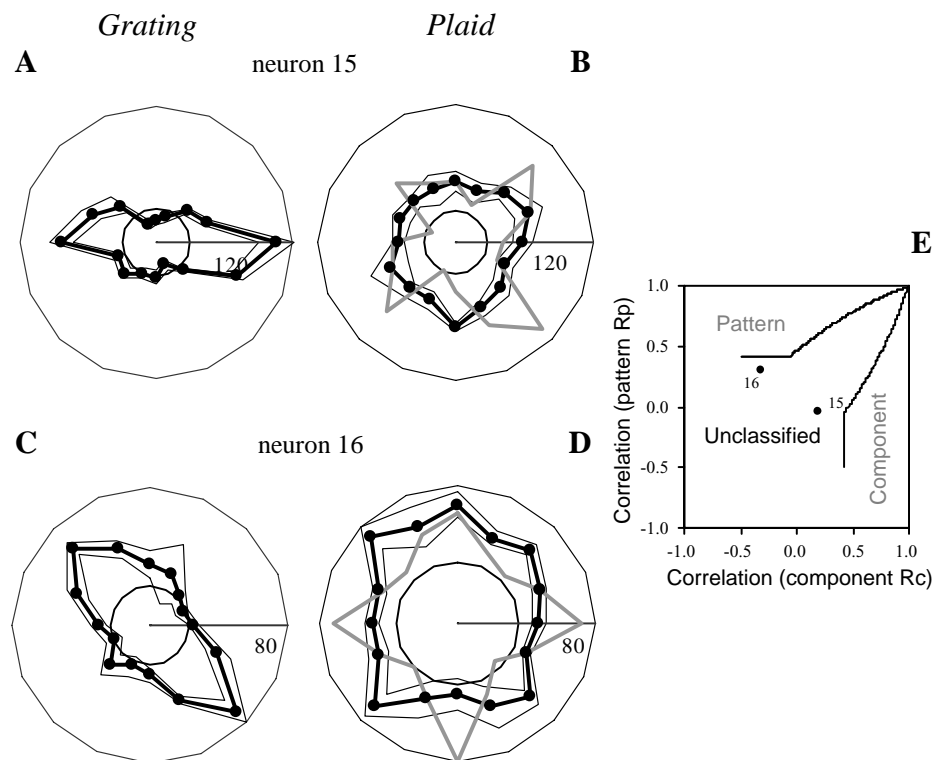


FIG. 7. Direction/orientation tuning curves to drifting gratings (A and C) and plaids (B and D) of two bi-direction selective neurons termed as unclassified neurons. The scatter plot diagram of the distribution of two neurons' partial correlation coefficients is shown in E.

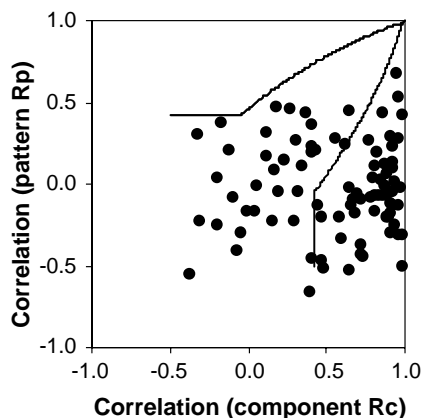


FIG. 8. Distribution of partial correlation coefficients (R_p and R_c) for bi-direction selective neurons sampled in area V1 of behaving monkeys.

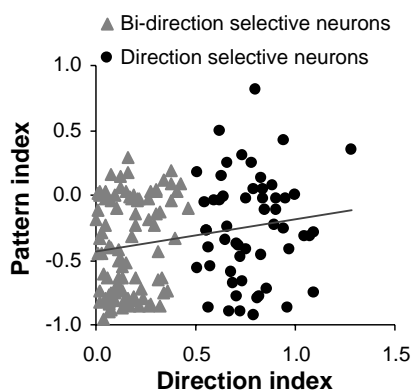


FIG. 9. Distribution of the strength of pattern motion selectivity (pattern index) and direction selectivity (direction index) for direction and bi-direction selective neurons sampled in area V1 of behaving monkeys.

most V1 neurons projecting to MT terminate in layer IV (Maunsell & Van Essen, 1983; Ungerleider & Desimone, 1986; Shipp & Zeki, 1989) and are CM selective (Movshon & Newsome, 1996), a local hierarchical scheme has been suggested in which V1 component neurons feed into MT component neurons. The latter may in turn project to pattern neurons (Stoner & Albright, 1994).

A similar hierarchical pathway has also been observed in the cortex of anaesthetized cats. Almost all direction selective neurons in striate cortex and lateral suprasylvian cortex showed clear CM selectivity (Gizzi *et al.*, 1990), while 55% of direction selective neurons in the higher area (anterior ectosylvian visual area) of the assumed serial hierarchy were classified as PM selective (Scannell *et al.*, 1996).

These findings confirmed the existence of the hierarchical motion processing system. In the primary motion detection stage (area V1), direction selective neurons act as local motion energy filters (Adelson & Bergen, 1985; Grzywacz & Yuille, 1990) and respond to the motion of image constituents within particular bandpass characteristics for orientation, spatial and temporal frequency. These neurons therefore simply encode the motion of the orientated components comprising a complex pattern rather than the global motion of the pattern itself. Neurons in the later motion integration stage (area MT) perform more complex computations based on extensive local motion measurements provided by V1, and detect the true direction of global motion that is independent of the motion of contours within them (Movshon *et al.*, 1985; Movshon & Newsome, 1996).

Although most V1 direction selective neurons recorded in awake, fixating monkeys were CM selective (as classically described in anaesthetized animals), we observed a small number of neurons (9%) that were clearly PM selective, and the population as a whole (especially for neurons recorded in layer 4B) is biased towards PM selective (Fig. 5A). This suggests that some V1 neurons can represent information about perceptual interpretation of locally derived motion/pattern signals. When tested with second-order motion stimuli (i.e. flicker-defined square wave grating drifting over a static texture, dynamic noise bar on static noise backgrounds), some neurons in macaque V1 showed similar direction selectivity to first-order motion stimuli (i.e. drifting sinusoidal grating and luminance defined bar) (Chaudhuri & Albright, 1997; O'Keefe & Movshon, 1998). In light of this, a natural interpretation is that neurons in area V1 are not only specialized for conveying information of a low-level nature, such as orientation and spatial frequency of luminance contrast, but also represent and communicate signals that may contribute to pattern or higher-order motion processing. Therefore, V1 activity should be interpreted in a more global and possibly perceptual context (Gilbert, 1998).

The absence of PM selective neurons in area V1 of anaesthetized animals supports the idea that local and global processing in V1 could be based on different mechanisms. Lamme *et al.* (1998b) found that some aspects of global perception, such as figure-ground modulation, were only observable in V1 when the animal was conscious. When

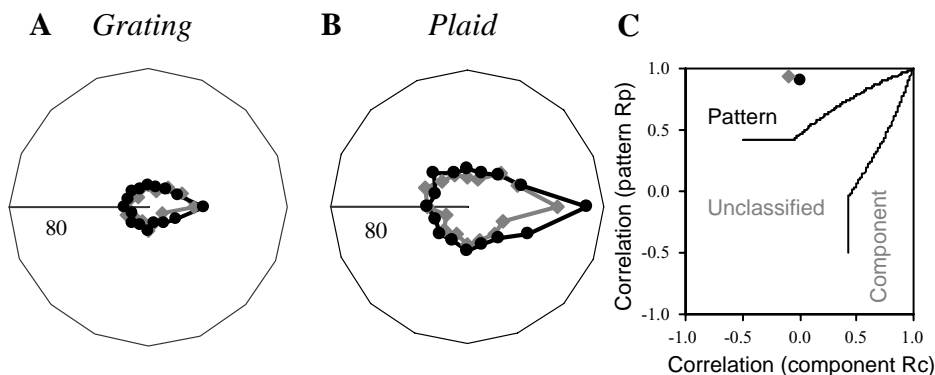


FIG. 10. Directional tuning curves of neuron 4 to drifting gratings (A) and plaids (B). The scatter plot diagram of its directional selectivity is shown in C. Black lines and symbols represent its responses sampled from the whole period of motion presentation; grey lines and symbols indicate its responses sampled from the time window between 200 and 1000 ms after the motion onset.

recording was repeated in anaesthetized animals, figure-ground related modulatory activity was selectively suppressed. Therefore, the perceptual interpretation in V1 might depend much more critically on information integration mechanisms that only function properly in awake, perceiving animals. One of these mechanisms might be feedback from extrastriate areas.

Neuroanatomical studies have shown that area V1 in macaque receives feedback connections from a number of extrastriate areas including V2, V3, V3A, V4, MT, PO and PIP (Felleman & Van Essen, 1991; Budd, 1998). The density of such back-projections, sometimes involving as many axons as in the forward pathway, suggests that they may exert a modulatory influence over V1 computations (Douglas & Martin, 1991; Lamme *et al.*, 1998a). Those feedback influences from neurons with larger RF and complex computation capabilities may inform V1 neurons the processing results of higher areas, and allow them to integrate some global information (Hochstein & Ahissar, 2002), such as context information (Zipser *et al.*, 1996; Gilbert, 1998), figure-ground segregation (Hupé *et al.*, 1998; Lamme *et al.*, 1998b), and attentive and conscious scene analysis (Lamme & Spekreijse, 2000; Lee *et al.*, 2002). Indeed, reversible inactivation of area MT showed feedback connections from MT have a facilitatory effect on the responses of V1 neurons to motion-based figure-ground segregation (Hupé *et al.*, 1998, 2001). For pattern motion selectivity, the back-projections from the output layers of MT, the layers containing high concentrations of PM selective neurons, terminate in layer IVB of V1 (Maunsell & Van Essen, 1983; Shipp & Zeki, 1989). As the PM selective neurons we recorded in V1 were distributed around putative layer IV, there is a strong possibility that these neurons might receive the critical feedback information from MT and thus inherit the computed property or properties of pattern motion selectivity so clearly evident in MT.

Acknowledgements

This study was supported by the UK Medical Research Council (MRC), the Oxford MRC Centre in Brain and Behaviour, the Oxford McDonnell-Pew Centre for Cognitive Neuroscience, and the US Air Force Office of Scientific Research (AFSOR) European Office of Aerospace Research and Development (EOARD). We thank the reviewers for their comments on the study.

Abbreviations

CM, component motion; DI, direction index; FP, fixation point; MT, middle temporal area; PM, pattern motion; *R_c*, partial correlation coefficient for component; RF, receptive field; *R_p*, partial correlation coefficient for pattern; SI, symmetry index.

References

- Adelson, E.H. & Bergen, J.R. (1985) Spatio-temporal energy models for the perception of motion. *J. Opt. Soc. Am. (a)*, **2**, 284–299.
- Adelson, E.H. & Movshon, J.A. (1982) Phenomenal coherence of moving visual patterns. *Nature*, **300**, 523–525.
- Andersen, R.A. (1997) Neural mechanisms of visual motion perception in primates. *Neuron*, **18**, 865–872.
- Barone, P., Bataidier, A., Knoblauch, K. & Kennedy, H. (2000) Laminar distribution of neurons in extrastriate areas projecting to visual areas V1 and V4 correlates with the hierarchical rank and indicates the operation of a distance rule. *J. Neurosci.*, **20**, 3263–3281.
- Blakemore, C. & Tobin, E.A. (1972) Lateral inhibition between orientation detectors in the cat's visual cortex. *Exp. Brain Res.*, **15**, 539–540.
- Budd, J.M.L. (1998) Extrastriate feedback to primary visual cortex in primates: a quantitative analysis of connectivity. *Proc. R. Soc. Lond. B*, **265**, 1037–1044.
- Carandini, M., Heeger, D.J. & Movshon, J.A. (1997) Linearity and normalization in simple cells of the macaque primary visual cortex. *J. Neurosci.*, **17**, 8621–8644.
- Chaudhuri, A. & Albright, T.D. (1997) Neuronal responses to edges defined by luminance vs. temporal texture in macaque area V1. *Vis. Neurosci.*, **14**, 949–962.
- Conway, B.R. & Livingstone, M.S. (2003) Space-time maps and two-bar interactions of different classes of direction-selective cells in macaque V1. *J. Neurophysiol.*, **89**, 2726–2742.
- DeValois, R.L., Yund, E.W. & Hepler, N. (1982) The orientation and direction selectivity of cells in macaque visual cortex. *Vision Res.*, **22**, 531–544.
- Douglas, R.J. & Martin, K.A.C. (1991) A functional microcircuit for cat visual cortex. *J. Physiol. (Lond.)*, **440**, 735–769.
- Dow, B.M. (1974) Functional classes of cells and their laminar distribution in monkey visual cortex. *J. Neurophysiol.*, **42**, 850–860.
- Felleman, D.J. & Van Essen, D.C. (1991) Distributed hierarchical processing in the primate cerebral cortex. *Cereb. Cortex*, **1**, 1–47.
- Ferrera, V.P. & Wilson, H.R. (1990) Perceived direction of moving two-dimensional patterns. *Vision Res.*, **30**, 273–287.
- Gegenfurtner, K.R., Kiper, D.C. & Levitt, J.B. (1994) Analysis of color and motion in macaque area V3. *Soc. Neurosci. Abstr.*, **20**, 1741.
- Gilbert, C.D. (1998) Adult cortical Dynamics. *Physiol. Rev.*, **78**, 467–485.
- Gizzi, M.S., Katz, E., Schumer, R.A. & Movshon, J.A. (1990) Selectivity for orientation and direction of motion of single neurons in cat striate and extrastriate visual cortex. *J. Neurophysiol.*, **63**, 1529–1543.
- Grzywacz, N.M. & Yuille, A.L. (1990) A model for the estimate of local image velocity by cells in the visual cortex. *Proc. R. Soc. Lond. (Biol.)*, **239**, 129–161.
- Guo, K. & Benson, P.J. (1998) Involuntary eye movements in response to first- and second-order motion. *Neuroreport*, **9**, 3543–3548.
- Guo, K. & Benson, P.J. (1999) Grating and plaid chrominance motion influences the suppressed ocular following response. *Neuroreport*, **10**, 387–392.
- Gur, M., Beylin, A. & Snodderly, D.M. (1997) Response variability of neurons in primary visual cortex (V1) of alert monkeys. *J. Neurosci.*, **15**, 2914–2920.
- Gur, M. & Snodderly, D.M. (1997) Visual receptive fields of neurons in primary visual cortex (V1) move in space with the eye movements of fixation. *Vision Res.*, **37**, 257–265.
- Hawken, M.J., Parker, A.J. & Lund, J.S. (1988) Laminar organization and contrast sensitivity of direction-selective cells in the striate cortex of the Old World monkey. *J. Neurosci.*, **8**, 3541–3548.
- Hochstein, S. & Ahissar, M. (2002) View from the top: hierarchies and reverse hierarchies in the visual system. *Neuron*, **36**, 791–804.
- Hubel, D.H. & Wiesel, T.N. (1962) Receptive fields, binocular interaction, and functional architecture in cat's visual cortex. *J. Physiol. (Lond.)*, **160**, 106–154.
- Hubel, D.H. & Wiesel, T.N. (1968) Receptive fields and functional architecture of monkey striate cortex. *J. Physiol. (Lond.)*, **195**, 215–243.
- Hupé, J.M., James, A.C., Girard, P., Lomber, S.G., Payne, B.R. & Bullier, J. (2001) Feedback connections act on the early part of the responses in monkey visual cortex. *J. Neurophysiol.*, **85**, 134–145.
- Hupé, J.M., James, A.C., Payne, B.R., Lomber, S.G., Girard, P. & Bullier, J. (1998) Cortical feedback improves discrimination between figure and background by V1, V2 and V3 neurons. *Nature*, **394**, 784–787.
- Judge, S.J., Richmond, B.J. & Chu, F.C. (1980) Implantation of magnetic search coils for measurement of eye position: an improved method. *Vision Res.*, **20**, 535–538.
- Lamme, V.A.F. & Spekreijse, H. (2000) Modulations of primary visual cortex activity representing attentive and conscious scene perception. *Front. Biosci.*, **5**, D232–D243.
- Lamme, V.A.F., Supér, H. & Spekreijse, H. (1998a) Feedforward, horizontal, and feedback processing in the visual cortex. *Curr. Opin. Neurobiol.*, **8**, 529–535.
- Lamme, V.A.F., Zipser, K. & Spekreijse, H. (1998b) Figure-ground activity in primary visual cortex is suppressed by anesthesia. *Proc. Natl. Acad. Sci. USA*, **95**, 3263–3268.
- Lee, T.S., Yang, C.F., Romero, R.D. & Mumford, D. (2002) Neural activity in early visual cortex reflects behavioural experience and higher-order perceptual saliency. *Nat. Neurosci.*, **4**, 533–539.
- Martinez-Conde, S., Macknik, S.L. & Hubel, D.H. (2002) The function of bursts of spikes during visual fixation in the awake primate lateral geniculate nucleus and primary visual cortex. *Proc. Natl. Acad. Sci. U.S.A.*, **99**, 13920–13925.
- Maunsell, J.H.R. & Van Essen, D.C. (1983) The connections of the middle temporal visual area (MT) and their relationship to a cortical hierarchy in the macaque monkey. *J. Neurosci.*, **3**, 2563–2586.
- Movshon, J.A., Adelson, E.H., Gizzi, M.S. & Newsome, W.T. (1985) The analysis of moving visual patterns. In Chagas, C., Gattass, R. & Gross,

- C.G. (Eds), *Study Group on Pattern Recognition Mechanisms*. Pontifica Academia Scientiarum, Vatican City, pp. 117–151.
- Movshon, J.A. & Newsome, W.T. (1996) Visual response properties of striate cortical neurons projecting to area MT in macaque monkeys. *J. Neurosci.*, **16**, 7733–7741.
- O'Keefe, L.P. & Movshon, J.A. (1998) Processing of first- and second-order motion signals by neurons in area MT of the macaque monkey. *Vis. Neurosci.*, **15**, 305–317.
- Orban, G.A. (1994) Motion processing in monkey striate cortex. In Peters, A. & Rockland, K.S. (Eds), *Cerebral Cortex, Primary Visual Cortex in Primates*, Vol. 10. Plenum Press, New York, pp. 413–441.
- Pack, C.C., Berezovskii, V.K. & Born, R.T. (2001) Dynamic properties of neurons in cortical area MT in alert and anaesthetized macaque monkeys. *Nature*, **414**, 905–908.
- Rodman, H.R. & Albright, T.D. (1989) Single-unit analysis of pattern-motion selective properties in the middle temporal visual area (MT). *Exp. Brain Res.*, **75**, 53–64.
- Salzman, C.D., Britten, K.H. & Newsome, W.T. (1990) Cortical microstimulation influences perceptual judgements of motion direction. *Nature (Lond.)*, **346**, 174–177.
- Scannell, J.W., Sengpiel, F., Tovée, M.J., Benson, P.J., Blakemore, C. & Young, M.P. (1996) Visual motion processing in the anterior ectosylvian sulcus of the cat. *J. Neurophysiol.*, **76**, 895–907.
- Schiller, P.H., Finlay, B.L. & Volman, S.F. (1976) Quantitative studies of single-cell properties in monkey striate cortex. I. Spatiotemporal organization of receptive fields. *J. Neurophysiol.*, **39**, 1288–1319.
- Shipp, S. & Zeki, S. (1989) The organisation of connections between areas V5 and V1 in macaque monkey visual cortex. *Eur. J. Neurosci.*, **1**, 309–332.
- Skottun, B.C., De Valois, R.L., Grosf, D.H., Movshon, J.A., Albrecht, D.G. & Bonds, A.B. (1991) Classifying simple and complex cells on the basis of response modulation. *Vision Res.*, **31**, 1079–1086.
- Snowden, R.J. (1994) Motion processing in the primate cerebral cortex. In Smith, A.T. & Snowden, R.J. (Eds), *Visual Detection of Motion*. Academic Press, London, pp. 51–83.
- Stoner, G.R. & Albright, T.D. (1992) Neural correlates of perceptual motion coherence. *Nature*, **358**, 412–414.
- Stoner, G.R. & Albright, T.D. (1994) Visual motion integration: A neurophysiological and psychophysical perspective. In Smith, A.T. & Snowden, R.J. (Eds), *Visual Detection of Motion*. Academic Press, London, pp. 253–290.
- Thiele, A. & Stoner, G. (2003) Neuronal synchrony does not correlate with motion coherence in cortical area MT. *Nature*, **421**, 366–370.
- Tinsley, C.J., Webb, B.S., Barraclough, N.E., Vincent, C.J., Parker, A. & Derrington, A.M. (2003) The nature of V1 neural responses to 2D moving patterns depends on receptive-field structure in the marmoset monkey. *J. Neurophysiol.*, **90**, 930–937.
- Ungerleider, L.G. & Desimone, R. (1986) Cortical connections of visual area MT in the macaque. *J. Comp. Neurol.*, **248**, 190–222.
- Zipser, K., Lamme, V.A.F. & Schiller, P.H. (1996) Contextual modulation in primary visual cortex. *J. Neurosci.*, **16**, 7376–7389.